Magnetially Suspended Ball

EECS 460 Lab Assignment Report

Ran Jia, Yanqi Liu, Tianhao Shao, Yuan Miao
Department of EECS
University of Michigan
Ann Arbor, MI 48109

I. Introduction

In this report, we detailed the principle of operation and transfer function used to model the maglev test-bed system. We designed a PID controller in the feedback loop and a pre-compensator to stabilize the open-loop unstable maglev system and satisfy design specifications. After simulation with linearized and non-linear model of the maglev system, we conducted various performance test of our controller on the hardware maglev test-bed. The design process and experiment results are included in this report.

II. Controller Design

A. 1-DOF Controller Design

The root locus of the linearized plant open-loop transfer function is shown in the following figure:

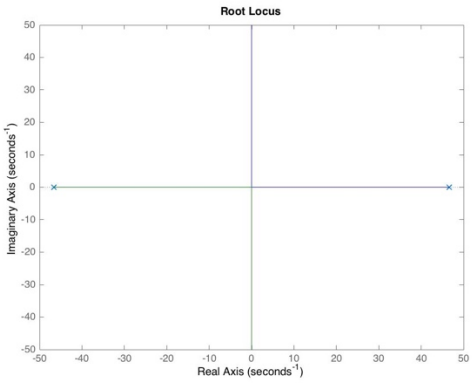

Figure 1: Root locus of linearized plant transfer function

From the root locus plot of plant transfer function, we can see that there is at least one pole in the right-half plane for all k. Therefore, we cannot achieve stability by increasing the gain k only.

According to the specifications, the desired damping ratio ζ is 0.6 and natural oscillating frequency ω_n is 1.67 so the desired pole is at -1+1.33i. The angle of deficiency is 0.071 degree.

We have initial design using a PD-PI cascaded controller. We design the PD controller at value $-7.78 * 10^{-3}(s + 808)$ to fix the transient response and PI controller of $\frac{s+0.1}{s}$ to fix the steady state error. The linearized Matlab model shows the response of linear system, which gives more overshoot than desired.

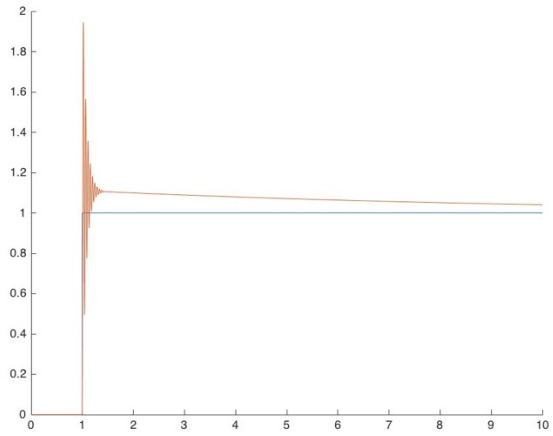

Figure 2: Step response of PI-PD controller

We also try to use a PID controller to achieve the design specification and stabilize the system. After trying out different values, we empirically determine the PID parameters K_P = -10, K_I= -1 and K_D = -2. This controller design stabilizes the system and gives the desired performance for linearized system. The simulation result and performance measurement is provided in section II.C.1.

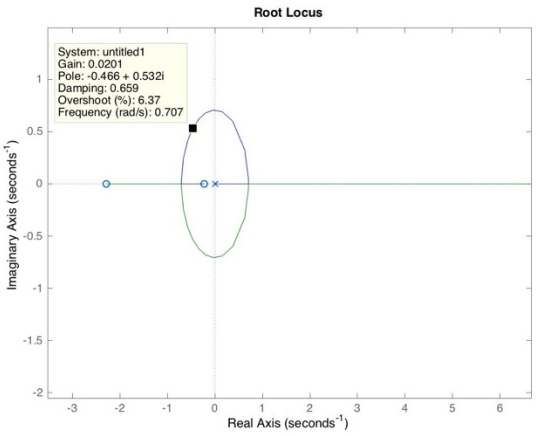

Figure 3: Root locus of PID controller

For the PID controller we design, close-loop stability could only be achieved at small magnitude of input ($10^{-6}\ cm$ range). The plot below shows the stable PID controlled non-linear model system response with $10^{-6}\ cm$ step input, and unstable response of the system with $10^{-5}\ cm$ step input.

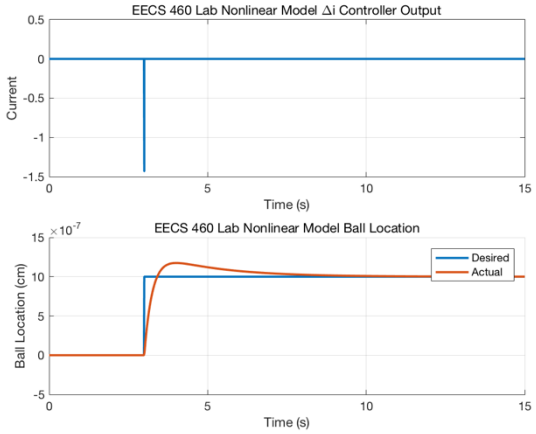

Figure 4: $10^{-6}\ cm$ stable step response of non-linear model

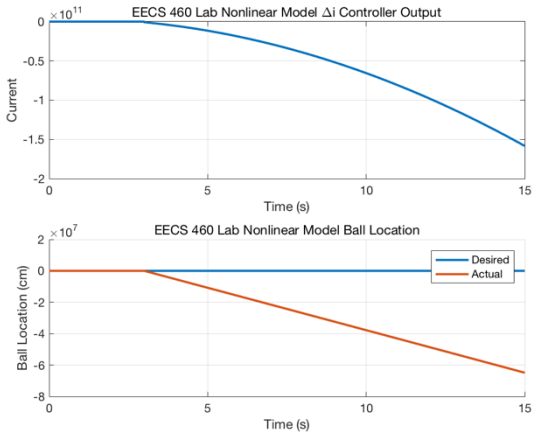

Figure 5: $10^{-5}\ cm$ unstable step response of non-linear model

Therefore, we need to use 2-DOF design to implement a proper pre-compensator to stabilize the system.

B. 2-DOF Controllers Design

From the 1-DOF linearized model simulation response, we can see that the controller output Δi, which is the current to electromagnet, is large at the moment when input switches. This factor reduces the robustness of our Maglev system and leads to the unstable nonlinear model simulation result in previous section.

To solve this problem and stabilize the Maglev system with larger size of command input, we need to design a pre-compensator to filter the high frequency component of input signal, and make the controller output less aggressive (low magnitude of Δi) to improve the robustness of our control system.

To achieve the desired result, we decide to design a 2nd order underdamped pre-compensator. We choose underdamped system because it ensures that the filtered signal will reach the step input magnitude within reasonable time interval. To filter out the high frequency component of the step command and smooth transition at controller input for small Δi, we choose the natural frequency $\omega_n = 2\ rad/sec$ and damping coefficient $\zeta = \frac{\sqrt{2}}{2} \approx 0.707$. We also choose the DC gain of our pre-compensator to be 1 so that the magnitude of input signal will not be affected. The transfer function of our pre-compensator is:

$$F(s) = \frac{\omega_n^2}{s^2 + 2\zeta\omega_n + \omega_n^2} = \frac{4}{s^2 + 2.828s + 4}$$

Simulation results of our 2-DOF controller design with both linearized and nonlinear model is presented in following section. Our 1-DOF PID controller design, along with our pre compensator design, meets the specification requirement.

C. Simulation Results with Linear Plant Model

1) 1-DOF controller

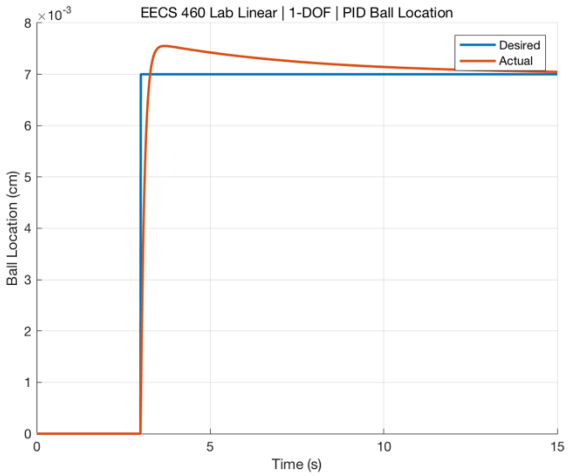

Figure 6: $\Delta y\ vs.\ \Delta t$ response with 1-DOF PID controller

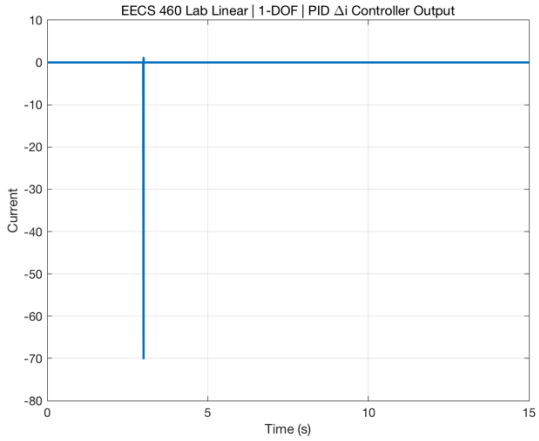

Figure 7: $\Delta i\ vs.\ \Delta t$ response with 1-DOF PID controller

From the step response of 1-DOF PID controller with linearized plant model, we calculated the following performance measures:

$e_{ss} \approx 0$ (With elongated simulation)
$5\%T_s = 5.865 - 3 = 2.865$ second
$\%Overshoot = \frac{0.755-(-0.7)}{0.7} * 100\% = 7.86\%$

The linearized system response with PID controller in loop meets the specification requirements.

2) 2-DOF controllers

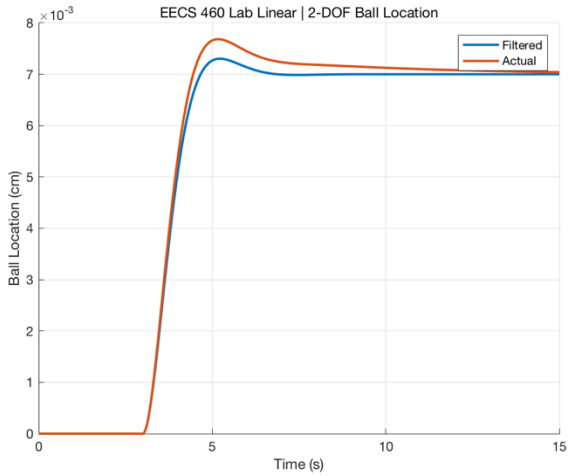

Figure 8: $\Delta y \; vs. \Delta t$ response with pre-compensator

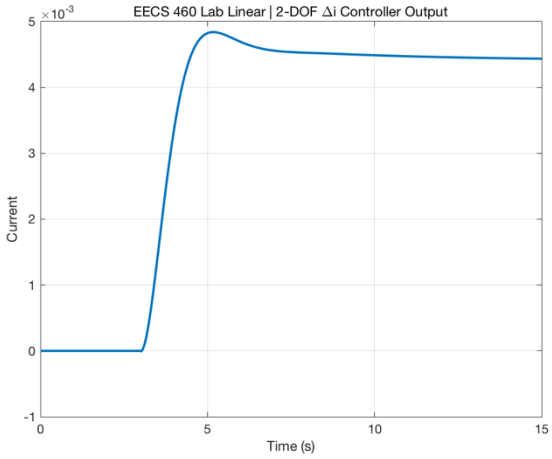

Figure 9: $\Delta i \; vs. \Delta t$ response with pre-compensator

From the step response of pre-compensator included system with linearized plant model, we calculated the following performance measures:

$e_{ss} \approx 0$ (With elongated simulation)
$5\%T_s = 6.311 - 3 = 3.311$ second
$\%Overshoot = \frac{0.768-(-0.7)}{0.7} * 100\% = 9.71\%$

The specification on settling time is slightly violated with pre-compensator due to the slower transition of filtered command input. The steady-state error and overshoot requirement is still satisfied with the pre-compensator. From the plot of controller output Δi, we can also see that the current output of controller is significantly reduced by degrees of magnitude, which is consistent with our design intention and increased robustness of our control system.

D. Simulation Results with Nonlinear Plant Model

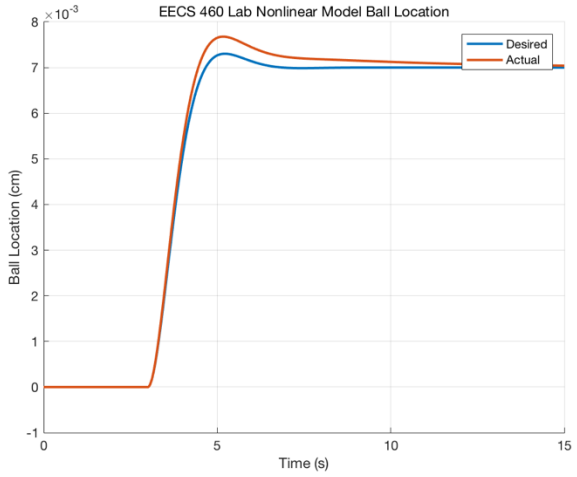

Figure 10: $\Delta y \; vs. \Delta t$ nonlinear response with pre-compensator

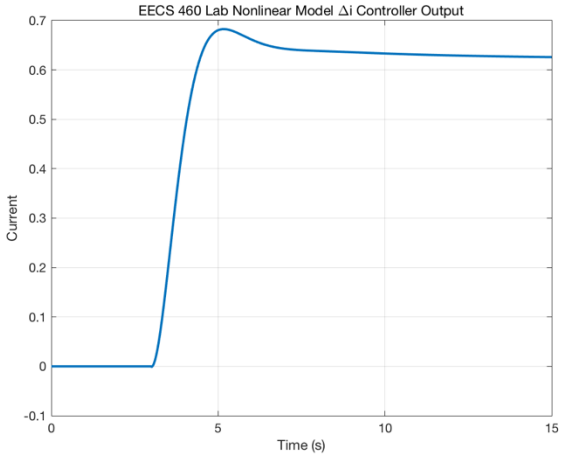

Figure 11: $\Delta i \; vs. \Delta t$ nonlinear response with pre-compensator

From the step response of pre-compensator included system with nonlinear plant model, we calculated the following performance measures:

$e_{ss} \approx 0$ (With elongated simulation)
$5\%T_s = 6.31 - 3 = 3.31$ second
$\%Overshoot = \frac{0.7677-(-0.7)}{0.7} * 100\% = 9.67\%$

The specification on settling time is slightly violated with pre-compensator due to the slower transition of filtered command input. The steady-state error and overshoot requirement is still met with nonlinear model. This also confirms that the linearized model is a good approximation for the system around normal operating point.

III. Experimental Setup

A. Experimental Apparatus

The sensor system of Maglev test-bed includes an infrared (IR) emitter-photodetector pair used to provide the relative position of levitated object. A non-inverting operational amplifier is used to amplify the photo-detector output signal.

The actuator of this system is the electromagnet, which is copper coils wrapped around an iron core. A power transistor is used to provide the driving current of the electromagnets to provide magnetic field.

The controller of this system uses the sensor signal as feedback to adjust the current through the electromagnet and levitate object to a close-loop stable location.

B. Principle of Operation

The photo-detector output voltage is related to the position of the levitated object, as its output voltage will increase when the levitated object falls. As the photo-detector output is directly proportional to the amount of infrared light sensed, the photo-detector output will be at maximum when there is no object under the coil, which provides maximum magnetic field and levitation force on the object from Ampere's Law. Under this circumstances, the object starts to raise and block the IR light, which leads to lower output of the photo-detector. This will continue until the object is levitated high enough that the output of photo-detector decrease to a sufficiently small value, which will turn off the transistor connected to the electromagnet. Then the object falls and the photo-detector begins to sense more light with higher output, which pulls up the object again and the cycle repeats.

C. Model of the Maglev System

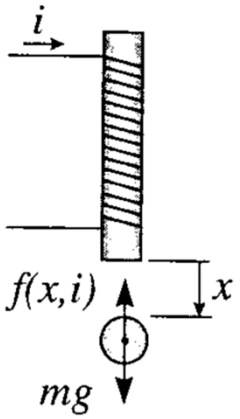

Figure 12: Free-body diagram of Maglev testbed

From the free-body diagram above, force exerted by the electromagnet on the levitated object is $f(x,i) = -\frac{i^2}{2}\frac{dL(x)}{dx}$ with total inductance $L(x) = L_l + \frac{L_0 x_0}{2}$, which is the sum of self-inductance of electromagnet and mutual inductance with the object. Combining the equation and linearizing around equilibrium I_0 and X_0 we have the following force equation:

$$f = C\left(\frac{I_0}{X_0}\right)^2 + \left[\left(\frac{2CI_0}{X_0^2}\right)i - \left(\frac{2CI_0^2}{X_0^2}\right)x\right] = f_0 + f_1, C = \frac{L_0 x_0}{2}$$

The incremental magnetic force $f_1 = f - f_0$ needs to be controlled. With the voltage-current relationship of electromagnet as $v = Ri + L_1\frac{di}{dt}$, and sensor as a gain element $v_s = k_s x$, we could solve the overall transfer function between input voltage of the electromagnet and output of sensor voltage as following:

$$G(s) = \frac{V_s(s)}{V(s)} = \frac{-\frac{2k_s C I_0}{mL_1 X_0^2}}{\left(s + \frac{R}{L_1}\right) * \left(s^2 - \frac{2CI_0^2}{mX_0^3}\right)}$$

IV. Experimental Results

The hardware implementation of maglev test-bed with Simulink constraints our choice of PID controller parameters. Therefore, we used $K_P = 4.5, K_I = 2$, and $K_D = 1$ for the hardware PID controller. The reduced PID gain parameter K_P may lead to longer settling time and extra overshoot in system response.

(All controller output Δi plots below use down-sampled data from lab measurements to ensure clarity of plots)

A. Stability

To test the stability of the system, we implement our PID controller in the feedback loop and pre-compensator according to our design. The system is stable with the default command input of $-1\ cm$, the response of system is shown in the following plot:

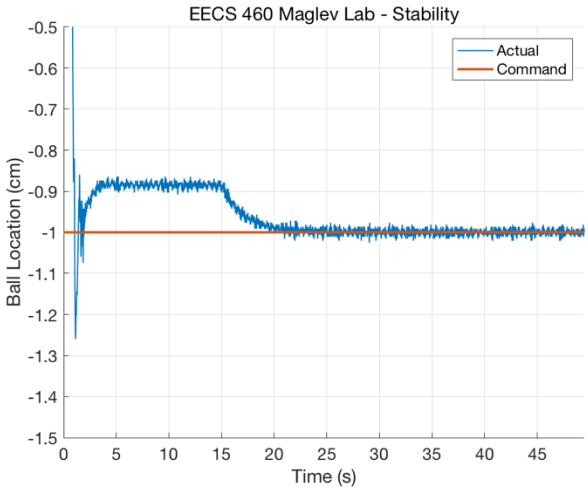

Figure 13: System response of constant input

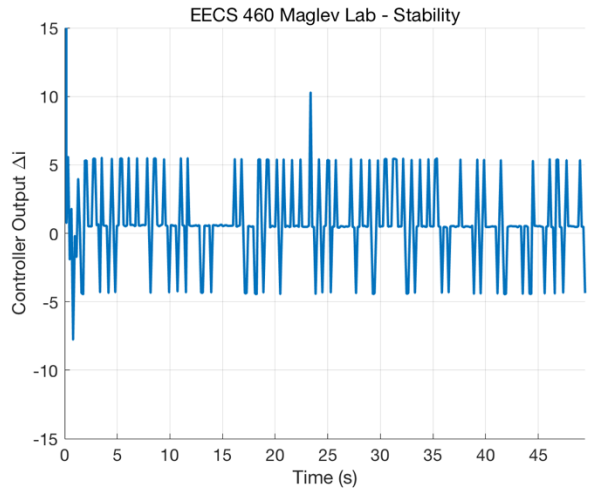

Figure 14: Controller output Δi of constant input

We can see that the system response is stable with constant command, and steady-state error is eliminated after 15sec when integration of PID is enabled.

B. Step Response

After the close-loop stability of our controller design verified in the previous part, we measure the performance of maglev system while tracking a step input. The system is configured with default step size of 0.4 cm relative to -1 cm initial position. The response of system is shown in the following plot:

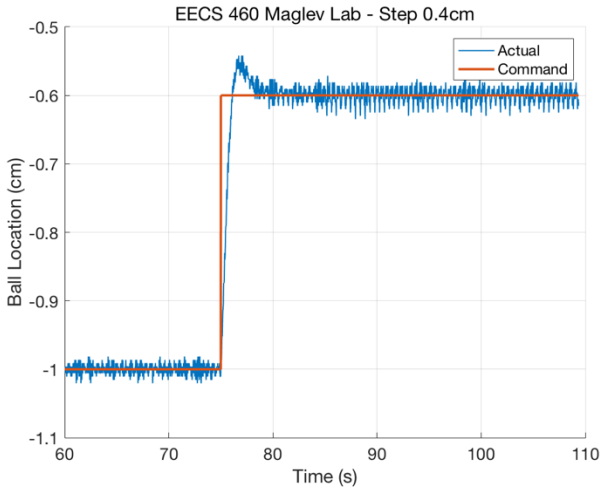

Figure 15: System response of 0.4cm step input

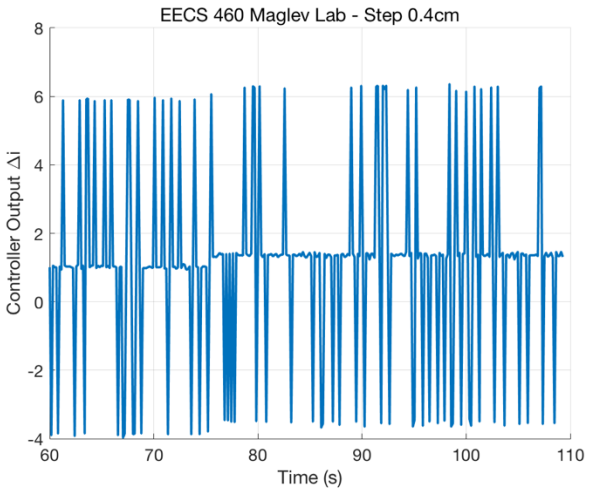

Figure 16: Controller output Δi of 0.4cm step input

Using the measurement data, we calculate the following performance parameter of this system:

$e_{ss} \approx 0$ (The actual ball location is oscillating around command value)
$5\% T_s = 77.96 - 75 = 2.96$ second
$\%Overshoot = \frac{-0.557-(-0.6)}{-0.6} * 100\% = 7.17\%$

We can see that our controller design for the maglev system meets all design specifications. And the controller output plot shows that the current is within reasonable range.

In addition to the default size of step input, we also use the largest step size of command signal that the feedback control system could track. After several attempts, we determine that the system could track input signal with step size up to 2.25 cm relative to -1 cm initial position. The response of system is shown in the following plot:

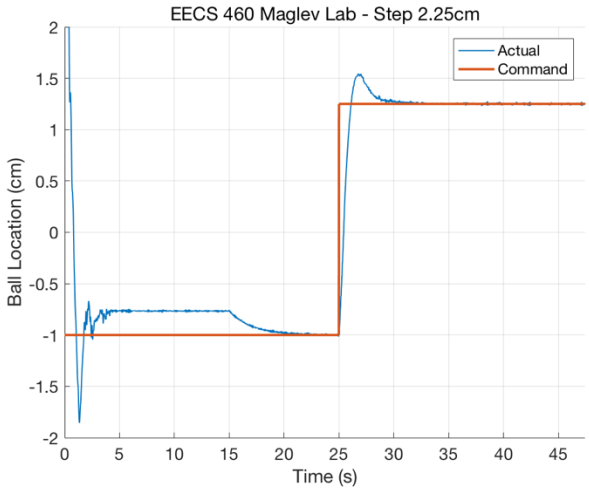

Figure 17: System response of 2.25cm step input

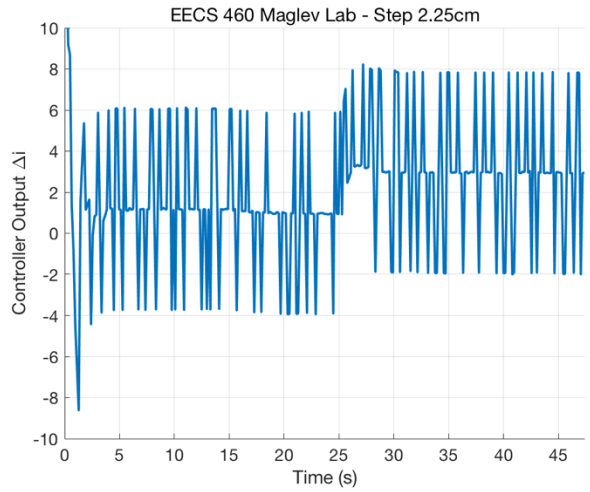

Figure 18: Controller output Δi of 2.25cm step input

Using the measurement data, we calculated the following performance parameter of this system:

$e_{ss} \approx 0$
$5\%T_s = 28.3 - 25 = 3.3$ second
$\%Overshoot = \frac{1.53-(1.25)}{2.25} * 100\% = 12.4\%$

The performance of the system degrades slightly below design specifications with large input signal changes, but the system is still stable. The controller output plot shows that the average level of controller output change when input step is larger with larger magnitude of step command, this is consistent with our expectation.

C. *Disturbance Rejection*

In this part of experiment, we test the disturbance rejection performance that relates to robustness of our controller design. We perform this test by perturbing the metal ball off its equilibrium position by hand, while the system is stable and tracking constant input. This movement applied approximately 1.5cm disturbance of ball location to the system. The response of system is shown in the following plot:

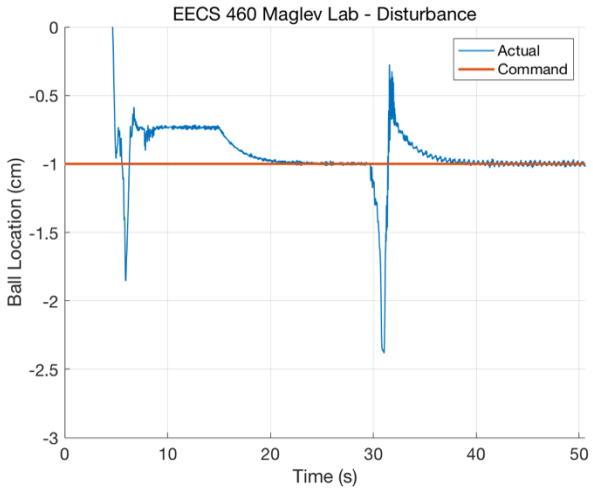

Figure 19: System response with disturbance

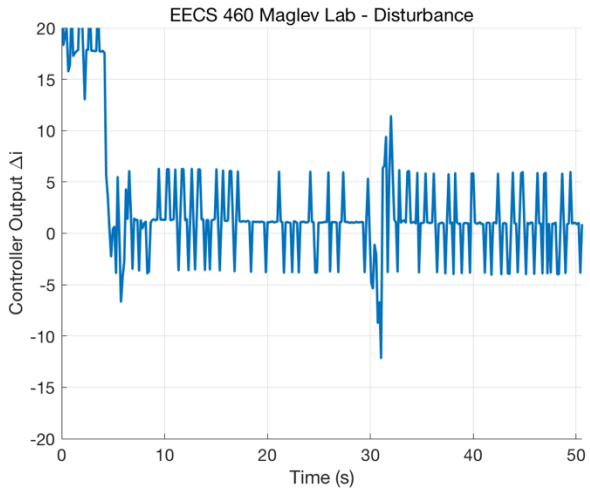

Figure 20: Controller output Δi with disturbance

From the plot above, we see that the system rejects the disturbance effectively. The close loop controlled maglev system corrects ball position to command signal with no steady-state error. The 5% settling time after the disturbance applied is approximately 4sec, which is close to the design specification of step input. The only potential problem is the overshoot after the disturbance, which might be the result of derivative component of PID in respond to abrupt changes.

D. *Staircase Waveform Tracking*

In this part of experiment, we test the ability of our controller to track the provided 5-level staircase waveform as command input. The response of system is shown in the following plot:

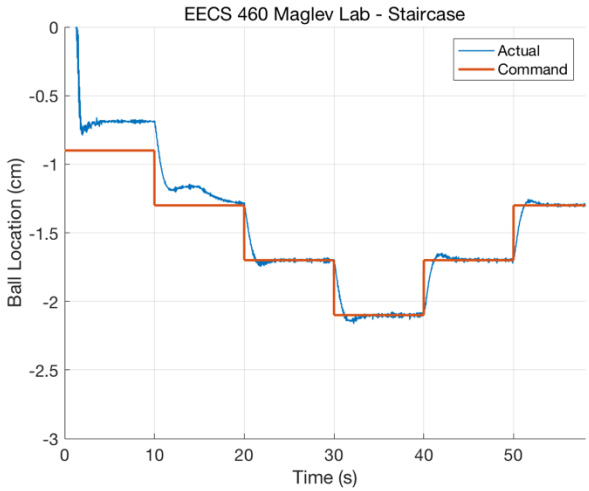

Figure 21: System response of staircase waveform

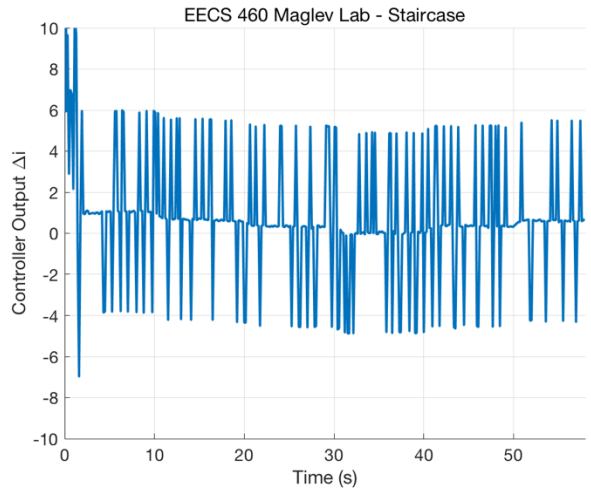

Figure 22: Controller output Δi of staircase waveform

From the plot above, we see that the system can track the 5-level staircase waveform without problem. The steady-state error is eliminated after 15sec when integration of PID is enabled. The 5% settling time after each level of staircase is equal or less than 3sec, which meets the specification. The maximum percentage overshoot is approximately 4%, which occurs at the final stair level of $-1.2\ cm$. Therefore, all design specifications are met with staircase waveform input.

E. Square Waveform Tracking

The final part of this experiment is to test how well could our designed controller track a 1/8 Hz square wave. We started with a square wave with an amplitude 0.6cm. The response of system is shown in the following plot:

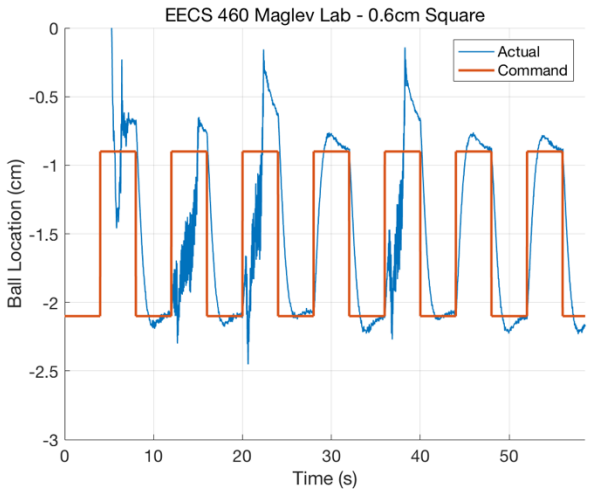

Figure 23: System response of 0.6cm square waveform

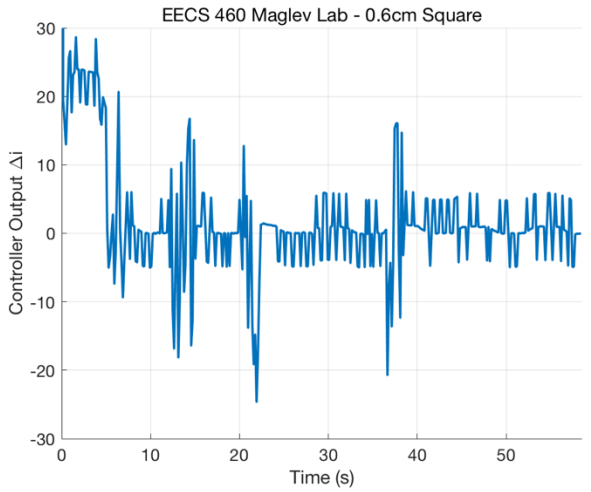

Figure 24: Controller output Δi of 0.6cm square waveform

From the plot of the system response above, the maglev system with our controller design could track 0.6cm magnitude square waveform. Although during the early transition the system shows excessive oscillation due to the initialization of integrator and causing large overshoot in early cycles, the system response eventually stabilizes and achieves zero steady-state error at the end of cycle. From the measurement data, the system response has an overshoot of 0.12cm magnitude during the stabilized cycles, and a 5% settling time around 4sec, which is close to our design specification.

In addition to the default magnitude of square waveform, we also test the largest square waveform that the maglev control system could track. After several attempts, we determine that the system could track a square waveform with magnitude up to $0.7\ cm$. The response of system is shown in the following plot:

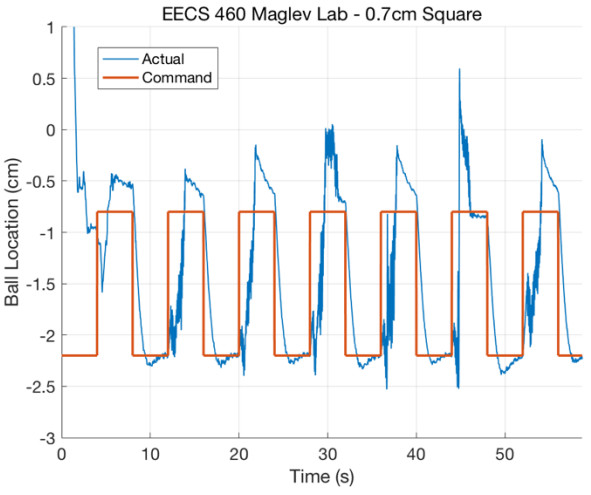

Figure 25: System response of 0.7cm square waveform

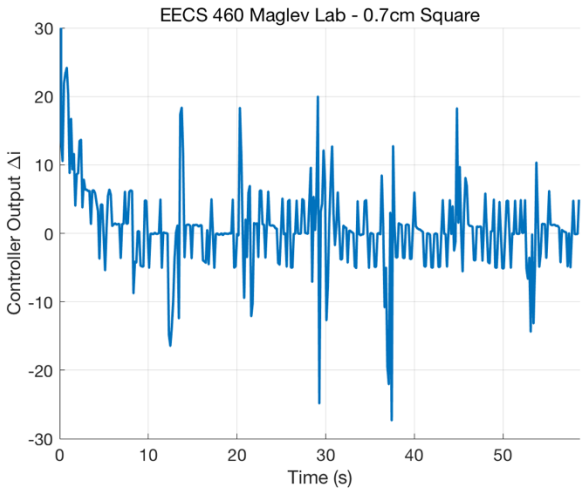

Figure 26: Controller output Δi of 0.7cm square waveform

Although the performance of the system degrades at large magnitude of square waveform, our controller design can still track the square waveform at 0.7cm without unstable system response. The large and frequent change of command signal leads to large overshoot and, during some cycles, actual ball position cannot reach the command value in time.

V. Conclusion

All the lab assignments are completed by our group. The designs of our 1-DOF and 2-DOF controller satisfy most of the related design specification, which are proved by the experimental results shown above in section IV. Like the way we were lectured, we first determined the transfer function of the original system and then designed a controller according to the specific requirements using root locus and other design methods. Since the system model provided to us is accurate on representing the Maglev system dynamics and our group prepared well before the lab, our group did not meet unexpected challenges while performing measurements. In terms of recommendation for future class, it would be more beneficial if we could get some basic knowledge about all the components and features of Simulink, thus we could design the controller system without encountering difficulties.

Appendix - Contributions

Yanqi Liu: Design the 1-DOF PD-PI cascaded controller and PID controller, and draft the relative report sections.

Ran Jia: Design the pre-compensator to implement 2-DOF PID controller, measure the required experiment data and draft the relative report sections.

Yuan Miao: Evaluate the measurement data and draw the conclusion of our design.

Tianhao Shao: Evaluate the measurement data and revise the lab report draft.